IEEE Workshop on Applications of Computer Vision, Nov. 30 - Dec. 2, 1992, Palm Springs, CA.

# New Visual Invariants for Obstacle Detection Using Optical Flow Induced From General Motion

Gin-Shu Young[1,2], Tsai-Hong Hong[1], Martin Herman[1], and Jackson C. S. Yang[2]

[1]National Institute of Standards and Technology (NIST), Bldg 220, Rm B124, Gaithersburg, MD 20899

[2]Robotics Laboratory, Department of Mechanical Engineering, University of Maryland, College Park, MD 20742

## Abstract

*To operate autonomous vehicles safely, obstacles must be detected before any path planning and obstacle avoidance activity is undertaken. In this paper, a novel approach to obstacle detection has been developed. New visual linear invariants based on optical flow have been developed. Employing the linear invariance property, obstacles can be directly detected by using a reference flow line obtained from measured optical flow. This method can be used for ground vehicles to navigate through man-made roadways or natural outdoor terrain or for air vehicles to land on known or unknown terrain. The main features of this approach are that (1) 2-D visual information (i.e., optical flow) is directly used to detect obstacles; no range, 3-D motion, or 3-D scene geometry is recovered; (2) knowledge about the terrain model, camera-to-ground coordinate transformation, or vehicle (or camera) motion is not required; (3) the method is valid for the vehicle (or camera) undergoing general six-degree-of-freedom motion; (4) the error sources involved are reduced to a minimum, since the only information required is one component of optical flow. Four initial experiments using both synthetic and real image data are presented.*

## 1 Introduction

To operate autonomous vehicles safely, obstacles must be detected before any path planning and obstacle avoidance activity is undertaken. Obstacles are defined as any region in space where a vehicle should not or cannot traverse, such as protrusions (objects lying on top of the terrain), depressions (potholes, ruts, gullies in the terrain), or steep terrain (shown in figure 1). The goal of this paper is to develop a simple, robust, and general method for obstacle detection by ground vehicles or during air vehicle landing. The vehicle can move under general motion, i.e., arbitrary translation and rotation. The method developed allows the ground vehicle to navigate through man-made roadways or natural outdoor terrain. The method also allows the aircraft to land on known or unknown terrain.

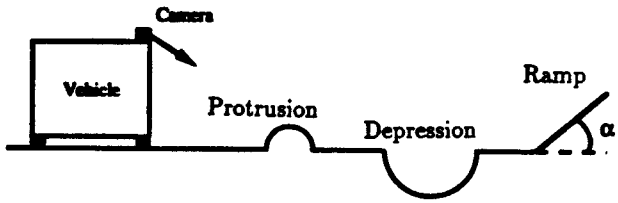


Fig. 1 Terrain with obstacles

For many applications in computer vision, it is important to recover range, 3-D motion, and/or 3-D scene geometry from a sequence of images [7] [22]. Most existing methods perform obstacle detection based on *range information* [2] [3] [4] [6] [9] [20] [23]. However, it is possible to detect obstacles by extracting relevant 2-D information from the imagery and using this information directly, without 3-D reconstruction. For example, in [24], we developed a new approach using optical flow without recovering range, 3-D motion, and/or scene geometry. For terrain characterization, slopes of surface regions were calculated *directly* from optical flow and some error analysis was also done in [25]. However, the method in [24] [25] is limited to translational camera motion. In this paper, new visual invariants for obstacle detection using optical flow are introduced and the method is valid for general six-degree-of-freedom motion.

Optical flow is the two dimensional motion in the camera image plane. The optical flow results from the relative motion between the camera and objects in the environment and represents the apparent mo-

tion of object points through a sequence of images. For sideward-looking camera motion, objects that are close to the camera will appear to flow faster than objects that are distant. However, this rule is not valid for general camera motion. This means that the flow field due to general motion is much more complex than for pure translation motion.

Optical flow, used by many biological creatures for navigation [1] [13], can provide very powerful information for vision-based navigation. Herman and Hong [8] have described how optical flow can be used to perform real-time navigation, during both teleoperated low data rate driving and autonomous driving. One of the main advantages of using optical flow is that the ratio of distance to speed (e.g., time-to-collision, visual looming) can be obtained and used for obstacle avoidance [11] [17]. Another advantage is that passive sensors (cameras), rather than active sensors such as laser scanners, are used. This eliminates radiation, reduces cost, and increases flexibility for many applications.

In this paper, new visual invariants are developed as a tool for obstacle detection. These invariants involve the mapping of points that lie on any straight line in 3-D space into an image-based space, i.e., a space whose coordinate axes represent parameter values extracted from the image domain. There are certain image-based spaces such that straight lines in 3-D space which are mapped to them *always* result in straight lines in the image-based space. We describe such a mapping as invariant for linear relationships, or simply linearly invariant, since linear relationships are always preserved. For example, we will show (see figure 2) that *a straight line* in 3-D space is *always a straight line* in the image-based space whose coordinates are x, $\dot{y}$ where x is the image position at the image line y=$y^*$ and $\dot{y}$ is the y component of optical flow. We will demonstrate that this type of visual invariant allows us to detect obstacles using optical flow. We will also demonstrate that if the linear relationship is not maintained in the image-based space, then it is difficult to detect obstacles in that space, i.e., the mapping must be linearly invariant. The features of our method are that:
**(1)** 2-D visual information (i.e., optical flow) is directly used to detect obstacles; no range, 3-D motion, or 3-D scene geometry is recovered;
**(2)** no information about the pose of the camera relative to the ground is required;
**(3)** no terrain model is required; and
**(4)** no information about the vehicle (or camera) motion is required.

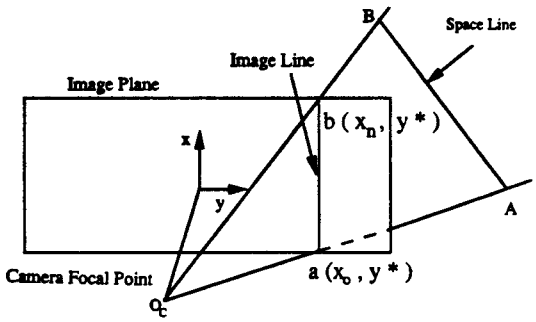


Fig. 2a Space line and image line

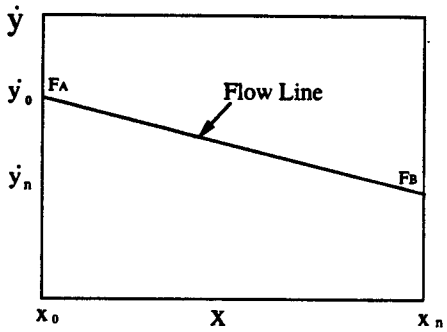


Fig. 2b Flow line in an image-based space

Fig. 2 A line in space mapping into a line in an image-based space

In the following, previous work is first discussed. Then, coordinate frames and a transformation matrix are introduced. Next, new visual invariants are developed. Following that the obstacle detection method based on these visual invariants is described. Finally, results using both synthetic and real image data are presented.

## 2 Previous Work

A number of obstacle detection methods have been developed in the past (e.g., [2] [3] [4] [5] [6] [9] [14] [15] [18] [19] [20] [21] [23]). Range information is often employed to solve this problem. This information may be obtained from active sensors (such as laser scanners, radars, and ultrasonics), stereo cameras, optical flow, etc. *A priori* knowledge is required by most existing methods. Such knowledge may include sensor-to-ground coordinate transformations, sensor motion, model optical flow fields, road models (or maps), etc. Errors in *a priori* knowledge result in errors in the output.

Some obstacle detection methods based on optical flow have been developed. Sridhar *et al* [20] at NASA

Ames Research Center investigated the methodology for obstacle detection for rotorcraft low altitude flight. The obstacle detection problem is posed as the problem of finding range to all objects in the field of view. Range information is obtained by the use of optical flow in their method. Bhanu et al [2] presented an inertial sensor integrated optical flow technique for motion analysis, in which range information is extracted from optical flow for obstacle detection. The method by Hoff and Sklair [9] detected landing hazards for a descending spacecraft, in which an algorithm using range information retrieved from optical flow with known camera motion was developed. Using flow field divergence, Nelson [14] detected discrete obstacles in free space other than on the terrain. Enkelmann [5] detected obstacles by evaluating the difference between calculated optical flow and estimated model flow. The estimated model requires knowledge about the focus of expansion (FOE), the transformation matrix between the camera and vehicle coordinate systems, and the camera motion. In addition, this method works only with a camera translating on a planar surface. Raviv [16] detected obstacles from an optical-flow-based invariant with an assumption of an observer that undergoes only translational motion in parallel to a planar surface. Mallot *et al* [12] detected discrete obstacles by the use of inverse perspective mapping. This method requires a coordinate transform and has the limitation of the observer (i.e., the camera) moving in the horizontal plane under pure translation.

The previous work described above is characterized by the following:
**(1)** range information extracted from optical flow, stereo, or active range sensors is often employed to detect obstacles,
**(2)** the observer's motion is often limited to translational motion in detecting obstacles directly from optical flow.
**(3)** *a priori* knowledge such as coordinate transformations, sensor motion, model optical flow fields, or road models (or maps) is often required.

## 3 Coordinate Frames and Transformation Matrix

Two coordinate frames important in our approach are the camera coordinate frame and the coordinate frame attached to a line in space. In this section, the two coordinate frames and the transformation matrix between them are introduced.

Consider the arbitrary line $\overline{AB}$ in space and its projection onto the image plane, line $\overline{ab}$ and say that image axis x is parallel to line $\overline{ab}$(figure 3). A coordinate frame c attached to the camera is chosen as follows:
**(1)** Let the camera focal point be the origin $O_c$.
**(2)** Let the optical axis be the $Z_c$ axis.
**(3)** Choose $X_c$ and $Y_c$ to be parallel to the image axes $x$ and $y$, respectively.

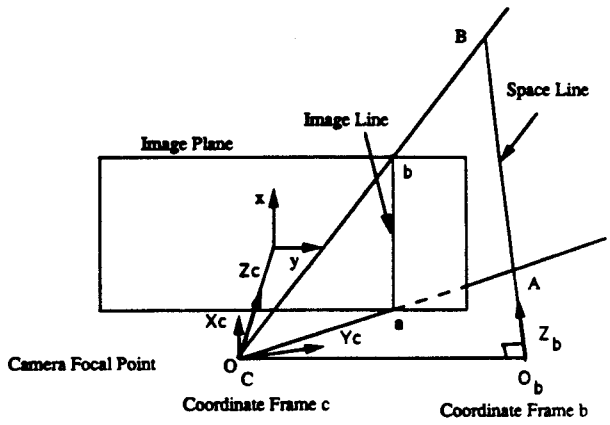


Fig. 3 Definition of two coordinate frames

A coordinate frame b is then affixed to the line $\overline{AB}$ as follows:
**(1)** Let the origin $O_b$ be the point lying on the extended line $\overline{AB}$ with the shortest distance from the camera focal point $O_c$.
**(2)** Let the $Z_b$ axis be line $\overline{AB}$.
**(3)** Choose $X_b$ and $Y_b$ arbitrarily as long as the right hand rule is obeyed.

A point P in the scene can be transformed from frame b to frame c by the equation:

$$\begin{Bmatrix} X_c \\ Y_c \\ Z_c \\ 1 \end{Bmatrix} = H_b^c * \begin{Bmatrix} X_b \\ Y_b \\ Z_b \\ 1 \end{Bmatrix} \tag{1}$$

where $(X_c, Y_c, Z_c)$ and $(X_b, Y_b, Z_b)$ are the coordinates of point P in frames c and b, respectively, and

$$H_b^c \equiv \begin{bmatrix} h_{11} & h_{12} & h_{13} & h_{14} \\ h_{21} & h_{22} & h_{23} & h_{24} \\ h_{31} & h_{32} & h_{33} & h_{34} \\ 0 & 0 & 0 & 1 \end{bmatrix} \tag{2}$$

represents a 4x4 transform matrix from frame b to frame c. Note that, at each instance of time, $H_b^c$ is constant for all points in the scene.

## 4 Visual Invariants

A visual invariant is an unchanged visual property. In this section, several new visual invariants for linear relationships are developed. As described above, these invariants are mappings with the property that *a straight line* in 3-D space is *always* mapped into *a straight line* in the appropriate image-based space. Some basic equations for developing these invariants are introduced first. Then the invariants are developed for both camera motion along the x- axis and general camera motion.

The visual invariants in this paper are based on optical flow $\bar{F}$, which can be expressed as :

$$\bar{F}(x,y,t) = (\dot{x}(x,y,t), \dot{y}(x,y,t)) = F(x,y,t)\bar{u}_F \quad (3)$$

where ($x$, $y$) is the image position, t is the instance of time, $\dot{x}$ and $\dot{y}$ are the components of optical flow, and F and $\bar{u}_F$ are the magnitude and unit directional vector of optical flow, respectively.

From the pinhole camera model, if we let the focal length be unity, the image position ($x$, $y$) is

$$x = \frac{X_c}{Z_c} \quad (4)$$

$$y = \frac{Y_c}{Z_c} \quad (5)$$

As defined earlier, line $\overline{AB}$ coincides with the $Z_b$ axis, therefore any points lying on line $\overline{AB}$ always have

$$X_b = Y_b = 0 \quad (6)$$

**Camera motion along the x-axis**

We start off our analysis of visual invariants with this simple case. Although the results presented here are not novel, they will serve to unify and complete the analysis we do later on for general camera motion, since the scenario of camera motion along the x-axis is not handled by the general analysis. The equations for optical flow due to a camera translating in the $X_c$ direction are

$$\dot{x} = \frac{1}{Z_c}(-T_X) \quad (7)$$

$$\dot{y} = 0 \quad (8)$$

$$F = \dot{x} \quad (9)$$

where $Z_c$ is the depth of the object relative to the camera, and $T_X$ is the translational motion of the object centered coordinate system relative to the camera. Note that, for each instance of time, $T_X$ is a constant for all points lying on a rigid object.

With equations (1)(2)(4) and (6), the following linear relationship can be obtained from equation (7) for all image points lying on line $\overline{ab}$ (i.e., y=constant) that arise from points in the scene lying on line $\overline{AB}$:

$$\dot{x} = a_1 + a_2 x \quad (10)$$

where

$$\begin{aligned} a_1 &= \frac{h_{13}}{a_3} \\ a_2 &= \frac{-h_{33}}{a_3} \\ a_3 &= \frac{(h_{34}h_{13} - h_{14}h_{33})}{(-T_X)} \end{aligned} \quad (11)$$

For each instance of time, $h_{ij}$ (the components of $H_b^c$) and $T_X$ are constants. Therefore, for each instance of time, the values $a_1$, $a_2$, and $a_3$ are constants for all points on line $\overline{AB}$. Equation (10) represents a line in the $\dot{x}$ vs. $x$ image-based space corresponding to a line in 3-D space. This is a visual invariant for lines. Note that the line in the domain of $\dot{x}$ vs. $x$ can be estimated from two points in principle (say, ($x_1$, $\dot{x}_1$) and ($x_2$, $\dot{x}_2$)). This means that specific knowledge about the transformation matrix and camera motion is not required.

**General camera motion**

The equations for optical flow due to general camera motion (arbitrary translation and rotation) are

$$\dot{x} = \frac{1}{Z_c}(-T_X + xT_Z) + (xy\omega_X - (1+x^2)\omega_Y + y\omega_Z) \quad (12)$$

$$\dot{y} = \frac{1}{Z_c}(-T_Y + yT_Z) + ((1+y^2)\omega_X - xy\omega_Y - x\omega_Z) \quad (13)$$

$$F = (\dot{x}^2 + \dot{y}^2)^{\frac{1}{2}} \quad (14)$$

where $Z_c$ is the depth of the object relative to the camera, and ($T_X$, $T_Y$, $T_Z$) and ($\omega_X$, $\omega_Y$, $\omega_Z$) are the translational and rotational motion of the object centered coordinate system relative to the camera. Note that, for each instance of time, ($T_X$, $T_Y$, $T_Z$) and ($\omega_X$, $\omega_Y$, $\omega_Z$) are constants for all points lying on a rigid object. If one component, say $\dot{y}$, of optical flow is always zero for any image lines, this would belong to the case of the camera motion along the x-axis described above.

With equations (1)(2)(4) and (6), the following nonlinear relationship can be obtained from equation (12) for all image points lying on line $\overline{ab}$ (i.e., y=constant) that arise from points in the scene lying on line $\overline{AB}$:

$$\dot{x} = b_1 + b_2 x + b_3 x^2 \quad (15)$$

where $b_1$, $b_2$, $b_3$ are constants. Equation (15) represents a curve in the $\dot{x}$ vs. x image-based space corresponding to a line in 3-D space. This is *not* a visual invariant for linear relationships.

With equations (1)(2)(4) and (6), the following linear relationship can be obtained from equation (13) for all image points lying on line $\overline{ab}$ (i.e., y=constant) that arise from points in the scene lying on line $\overline{AB}$:

$$\dot{y} = a_1 + a_2 x \tag{16}$$

where

$$\begin{aligned} a_1 &= \frac{h_{13}}{a_3} + (1+y^2)\omega_X \\ a_2 &= \frac{-h_{33}}{a_3} - y\omega_Y - \omega_Z \\ a_3 &= \frac{(h_{34}h_{13} - h_{14}h_{33})}{(-T_Y + yT_Z)} \end{aligned} \tag{17}$$

For each instance of time, $h_{ij}$ (the components of $H_b^c$) and ($T_X$, $T_Y$, $T_Z$) and ($\omega_X$, $\omega_Y$, $\omega_Z$) are constants. Therefore, for each instance of time, the values $a_1$, $a_2$, and $a_3$ are constants for all points on line $\overline{AB}$. Equation (16) represents a line in the $\dot{y}$ vs. x image-based space corresponding to a line in 3D space. This is a visual invariant. Note that the line in the $\dot{y}$ vs. x image-based space can be estimated from two points in principle (say, ($x_1$, $\dot{y}_1$) and ($x_2$, $\dot{y}_2$)). This means that specific knowledge about the transformation matrix and camera motion is not required.

If we were to combine equations (14),(15), and (16), then the resulting F as a function of x would be nonlinear. This is *not* a visual invariant for linear relationships.

In summary, we see that a straight line in 3-D space can be mapped into either a straight line or a curve depending on the camera motion and the image-based space used for the mapping. This means that visual invariants can be found only by selection of the *proper* image-based space. For example, a straight line in the $\dot{x}$ vs. $x$ image-based space is found for camera motion along the x-axis while a curve is found for general camera motion. Thus, the mapping to $\dot{x}$ vs. $x$ is a linear invariant for camera motion along the x-axis, but not for general camera motion. A curve in the F vs. $x$ image-based space is found for general camera motion. Therefore, the mappings to F vs. $x$ is not visual invariants for general camera motion. However, a straight line is *always* found in the $\dot{y}$ vs. $x$ image-based space for general camera motion. In other words, if $\dot{y}$ is not equal to zero, the mapping to the $\dot{y}$ vs. $x$ space is linearly invariant for lines in 3-D space for arbitrary camera motion.

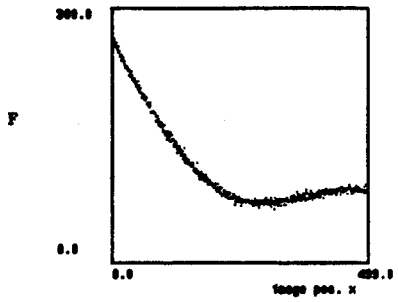


Fig. 4a F vs. $x$ without any obstacle

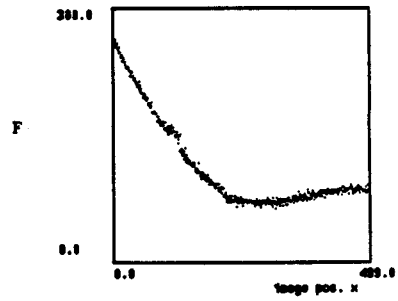


Fig. 4b F vs. $x$ with two obstacles

## 5 Obstacle Detection

The linear invariants found in the previous section are very useful for detecting discrete obstacles such as depressions or protrusions. Although the discussion thus far has been concerned only with single lines, many lines in the image plane can be processed in parallel to detect the full terrain ahead of the vehicle.

As described above, a mapping is a linear invariant only for certain image-based spaces. Only these mappings are useful for obstacle detection. To see this, consider the mapping to the F vs. $x$ image-based space, which is full flow magnitude F as a function of position x on the image line under consideration. This mapping is not a linear invariant. Figures 4a and 4b show the results of a simulation over two different types of terrain. The simulation involves 5 % noise added to the synthetic optical flow under general camera motion. Although no obvious differences can be observed between figures 4a and 4b, in figure 4a the terrain is flat and without obstacles, while in figure 4b the terrain has two obstacles, one protrusion and one depression. We see that obstacle detection can be very difficult in an image-based space that does not have the linear invariant property.

On the other hand, when an image-based space with the property of linear invariance is used, obsta-

cle detection becomes easy and straightforward. Consider the mapping to the $\dot{y}$ vs. $x$ image-based space, in which we consider only one component, $\dot{y}$, of optical flow as a function of $x$. This mapping is a linear invariant ( equation (16) ) under general camera motion. Figures 5a and 5b show the results of the same simulation, using the same camera motion and terrain, as in figures 4a and 4b, respectively. The mapping from points lying on a straight line in 3-D space looks like figure 2b. We call the line in figure 2b a reference line. Figure 5a appears to coincide with a reference line, implying that it is obtained from a terrain which is flat (at least in one dimension). Points that lie in the region in the image-based space above the reference line result from a protrusion on the terrain, while points that lie below the reference line result from a depression in the terrain. Thus in figure 5b, there are two obstacles, one a protrusion and the other a depression. Figure 5b can further be mapped into figure 5c where the reference line is horizontal. Figure 5c plots the difference between $\dot{y}$ and the y value of the reference line for each x value. A protrusion or a depression can easily be detected in figure 5c. Detailed experimental results are shown in the next section. To apply the property of linear invariance to obstacle detection, four steps are involved.

**Step 1:** Choosing an *arbitrary* straight line in the image.

This line intersects an image feature of interest, e.g., a potential obstacle. The chosen image line need not correspond to a linear feature in the scene.

**Step 2:** Estimation of the reference line for an image line.

This line can be obtained from the measured optical flow located in the lower image positions which correspond to regions on the ground surface near the vehicle. In principle, only two points are required to estimate the reference line.

**Step 3:** Computation of the difference.

The difference between the reference line obtained in **step 2** and the measured flow at all image positions lying on that image line is computed.

**Step 4:** Identification of obstacles.

The computed difference in **step 3** is used to detect obstacles. If the difference is larger than some threshold value, the observed point in space is considered to be an obstacle.

To detect obstacles easily, an image-based space with the property of linear visual invariance should be used. For arbitrary camera motion, the *proper* image-based space should be $\dot{y}$ vs. $x$ (or $\dot{x}$ vs. $y$) for any image line $y$=constant (or $x$=constant) if $\dot{y}$ (or $\dot{x}$) is not equal to zero. In the case where $\dot{y}$ (or $\dot{x}$) is always zero for any image lines, $\dot{x}$ vs. $x$ (or $\dot{y}$ vs. $y$) can be used.

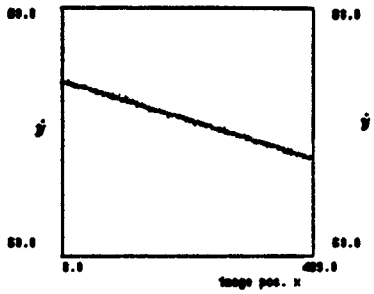

Fig. 5a $\dot{y}$ vs. $x$ without any obstacle

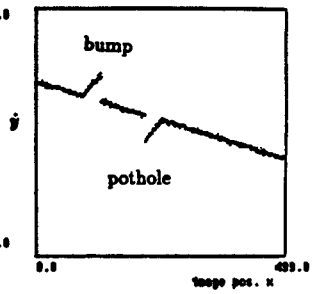


Fig. 5b $\dot{y}$ vs. $x$ with two obstacles

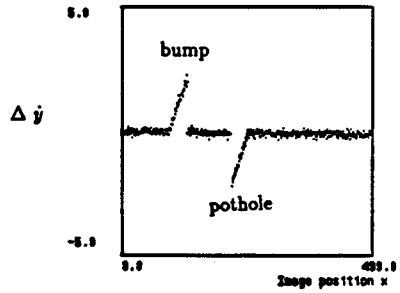


Fig. 5c $\Delta\ \dot{y}$ vs. $x$ with two obstacles

In this method, only one component of the optical flow is needed. Information such as a road or terrain model, specific knowledge of vehicle (or camera ) motion, or knowledge of the coordinate transformation between the camera and the ground is not required. Therefore the method reduces the error sources to a minimum since it employs minimum information. The approach is simple because obstacles are detected directly in the image-based space. Without any assumption of a terrain model, this method can be used for ground vehicles navigating in man-made roadways or natural outdoor terrain. This method can also be used for air vehicles undergoing general six-degree-of-freedom motion which are landing in known or unknown terrain.

## 6 Experimental Results

In this section, the results of four initial experiments demonstrating the simplicity and usefulness of linear invariants applied to obstacle detection are pre-

sented. The first two experiments are based on synthetic data with three different levels of noise, 5%, 10%, and 15%. In the experiments, the noise was generated randomly using a Gaussian distribution and was added to the optical flow obtained through simulation. This noise may represent the uncertainty value of the flow, potentially due to uneven terrain and/or unflat surfaces of objects in the environment. The last two experiments are based on real images taken in our laboratory. All results shown in this section are for one image line only. To cover the whole image, multiple image lines can be processed in parallel.

**Experiment 1**

The first experiment simulates a ground vehicle moving over terrain with a bump and a pothole, as shown in figure 6a. The bump is a semicircle which is 5.5 m ahead of the camera, with a height of 0.3 m above the flat terrain. The pothole is a semicircle which is 8.5 m ahead of the camera, with a depth of 0.6 m below the terrain. The camera is mounted on the top of the vehicle (2 m above the ground) and moves under a general motion with ($T_X$=-927, $T_Y$=-4 , $T_Z$=2853 mm/sec) and ($\omega_X$=0.05, $\omega_Y$=0.05, $\omega_Z$=0.05 rad/sec).

The results of experiments with 5% noise added to the synthetic optical flow have already been shown in figure 5c. Two obstacles, a protrusion and a depression can easily be detected from figure 5c. The results of experiments with noise of 10% and 15% are shown in figures 6b and 6c, respectively.

**Experiment 2**

This experiment simulates an air vehicle moving over terrain with multiple rectangular protrusions, as shown in figure 7a. The first protrusion is 34 m ahead of the camera with a height of 1 m above the flat terrain and the second protrusion is 50 m ahead of the camera with a height of 1.5 m above the flat terrain. The camera is mounted on the bottom of the air vehicle (20 m above the ground) and moves under a general motion with ($T_X$=-9270, $T_Y$=-40, $T_Z$=28530 mm/sec) and ($\omega_X$=0.05, $\omega_Y$=0.05, $\omega_Z$=0.05 rad/sec).

With 5%, 10%, and 15% noise added to the synthetic optical flow, the results of experiments are presented in figures 7b, 7c, and 7d, respectively.

**Experiment 3**

This experiment involves detecting a depression in a flat surface using real images. Figure 8a shows the lab setup, in which the camera is mounted on a linear positioning table and moves along a direction perpendicular to the camera's optical axis. This shows the case of camera motion along the x-axis. The camera moved with $T_X$ = 22.5 mm/s. A flat surface with a square depression of 50.8 mm is 406.4 mm ahead of the camera. The depression, located in the middle of the original image, is shown in figure 8b. Since $\dot{y} = 0$, we use the $\dot{x}$ vs $x$ image-based space which has the property of linear invariance. We consider only the scan line labeled in figure 8b. Optical flow at each pixel was obtained using a correlation method [10]. The values of optical flow $\dot{x}$ at image positions 40 through 199 are shown in figure 8c. The reference flow line can be obtained by fitting the data points near image position 40 to a line. The deviation of $\dot{x}$ from the reference flow line is shown in figure 8d. A depression can be easily detected in both figures 8c and 8d.

**Experiment 4**

This experiment is similar to experiment 3, except that the flat surface has a protrusion rather than a depression. The experimental setup is shown in figure 9a. The flat surface with the square protrusion of 76.2 mm is located at a distance of 469.9 mm from the camera. The protrusion, located in the left middle of the original image, is shown in figure 9b. The results are shown in figures 9c and 9d. detected.

## 7 Conclusion

In this paper, a novel approach to obstacle detection has been developed. New visual linear invariants based on optical flow have been found in the appropriate image-based spaces. Employing the linear invariance property, obstacles can be directly detected by using a reference flow line obtained from measured optical flow.

The approach has several advantages:

**(1) Simple** - Only one component of the optical flow is needed. Knowledge about the terrain model, coordinate transform, or vehicle (or camera) motion is not required. No range, 3-D motion, or 3-D scene geometry is recovered. 2-D visual information (i.e., optical flow) is directly used to detect obstacles. The feature used to detect obstacles is simple - a straight line.

**(2) General** - This approach is valid for the vehicle (or camera) moving under general motion, i.e., arbitrary translation and rotation.

**(3) Fast** - The method is simple and therefore computationally fast. Each image line can be processed in parallel.

**(4) Robust** - The error sources involved are reduced to a minimum since the only required information is one component of the optical flow. A reference flow line, as a feature used to detect obstacles, is obtained from measured optical flow. This avoids multiple er-

ror sources, such as one error source from measured data and another from model data.

Four initial experiments included in the paper suggest that the approach using visual linear invariants as a tool for obstacle detection is effective and robust.

An issue that has not been discussed here is how to find components of flow perpendicular to an arbitrary image line. We propose to do this by finding normal flow using spatiotemporal gradient methods, and then processing many lines in the image in parallel. Each line will, in general, contain only a few image points whose normal flow is perpendicular to the line. However, the sum of the image points that can be used with a large number of image lines should be dense enough to be useful for obstacle avoidance. We will pursue this in the future.

## 8 Acknowledgements

The authors would like to thank Dr. James Albus and Dr. David Coombs for important comments on this work.

## References

[1] J. S. Albus, T. H. Hong, "Motion, Depth, and Image Flow," *Proc. IEEE Int'l Conf. on Robotics and Automation*, 1990.

[2] B. Bhanu, B. Roberts, and J. Ming, "Inertial Navigation Sensor Intergated Motion Analysis for Obstacle Detection" *Proc. IEEE Int'l Conf. on Robotics and Automation*, 1990.

[3] M. J. Daily, J. G. Harris, and K. Reiser, "Detecting Obstacles in Range Imagery," *Proc. Image Understanding Workshop*, 1987.

[4] R. T. Dunlay and D. G. Morgenthaler, "Obstacle avoidance on roadways using range data," *SPIE Mobile Robots*, Vol. 727, 1986.

[5] W. Enkelmann, "Obstacle Detection by Evaluation of Optical Flow Fields," *First Europen Conf. on Computer Vision*, 1990.

[6] M. Hebert and T. Kanade, "3D Vision for Outdoor Navigation by an Autonomous Vehicle," *Proc. Image Understanding Workshop*, 1988.

[7] D. Heeger and A. Jepson, "Subspace Methods for Recovering Rigid Motion I: Algorithm and Implementation," *International Journal of Computer Vision*, in press.

[8] M. Herman and T. H. Hong, "Visual Navigation using Optical Flow," *Proc. NATO Defense Research Group Seminar on Robotics in the Battlefield*, Paris, France, March 1991.

[9] W. Hoff and C. Sklair, "Planetary Terminal Descent Hazard Avoidance Using Optical Flow ," *Proc. IEEE Int'l Conf. on Robotics and Automation*, 1990.

[10] H. Lau, "Optical Flow Extraction with Motion Known A priori," U. of Maryland, master thesis, EE dept., May 1992.

[11] D. N. Lee, "A theory of visual control of braking based on information about time-to-collision," *Perception*, Vol. 5, pp437-459, 1976.

[12] H. A. Mallot et al., "Inverse perspective mapping simplifies optical flow computation and obstacle detection," *Biological Cybernetics*, Vol. 64, pp177-185, 1991.

[13] K. Nakayama, "Biological Image Motion Processing: A Review," Vision Res., Vol. 25, No. 5, pp 625-660, 1985.

[14] R. C. Nelson and J. Aloimonos, "Obstacle Avoidance using Flow Field Divergence," *IEEE Transactions on PAMI*, Vol. 11, No. 10, Oct. 1989.

[15] D. N. Oskard, T. H. Hong, and C. A. Shaffer, "Real-Time Algorithms and Data Structures for Underwater Mapping," *IEEE Trans. on Systems, Man, and Cybernetics*, Vol. 20, No. 6, 1990.

[16] D. Raviv, "Flat Surfaces: A Visual Invariant," *NISTIR 4794*, NIST, Gaithersburg, MD, Mar. 1992.

[17] D. Raviv, "A Quantitative Approach to Looming," *NISTIR 4808*, NIST, Gaithersburg, MD, Apr. 1992.

[18] S. Singh and P. Keller, "Obstacle Detection for High Speed Autonomous Navigation," *Proc. IEEE Int'l Conf. on Robotics and Automation*, 1991.

[19] U. Solder and V. Graefe, "Object Detection in Real Time," *SPIE Vol. 1388 Mobile Robots V*, 1990.

[20] B. Sridhar, R. Suorsa and P. Smith, "Vision Based Techniques for Rotorcraft Low Altitude Flight," *SPIE* , Vol. 1571, 1991.

[21] K. Storjohann, T. Zielke, H. A. Mallot and W. Seelen, "Visual Obstacle Detection for Automatically Guided Vehicles," *Proc. IEEE Int'l Conf. on Robotics and Automation*, 1990.

[22] C. Tomasi and T. Kanade, "The Factorization Method for the Recovery of Shape and Motion from Image Streams," *Proc. Image Understanding Workshop*, 1992.

[23] P. A. Veatch and L. S. Davis, "Range Imagery Algorithms for the Detection of Obstacles by Autonomous Vehicles," *Center for Automation Research Technical Report*, CAR-TR-309, July 1987.

[24] G.-S. Young, T. H. Hong, M. Herman, and J. C. S. Yang, "Obstacle Detection for a Vehicle Using Optical Flow," *Intelligent Vehicles '92*, June 29 - July 1, 1992 in Detroit.

[25] G.-S. Young, T. H. Hong, M. Herman, and J. C. S. Yang, "Obstacle Detection and Terrain Characterization Using Optical Flow Without 3-D Reconstruction," SPIE Vol. 1825, Intelligent Robots and Computer Vision XI: Algorithms, Techniques, and Active Vision, Nov. 16 - 18, 1992, Boston, Ma.

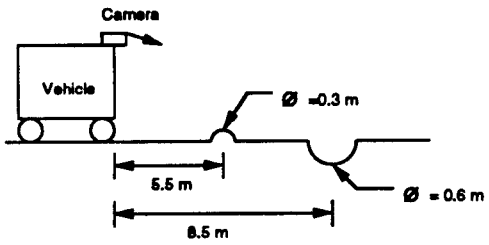


Fig. 6a Side view of terrain with a bump and a pothole

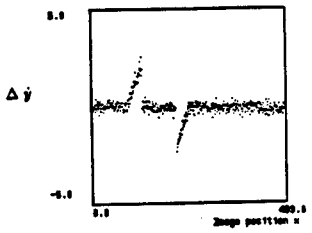

Fig. 6b $\Delta\ \dot{y}$ vs. $x$ in experiment 1 ( 10 % noise )

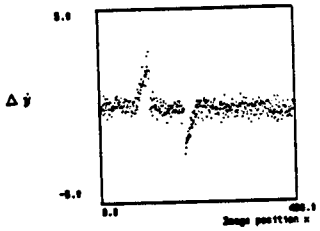

Fig. 6c $\Delta\ \dot{y}$ vs. $x$ in experiment 1 ( 15 % noise )

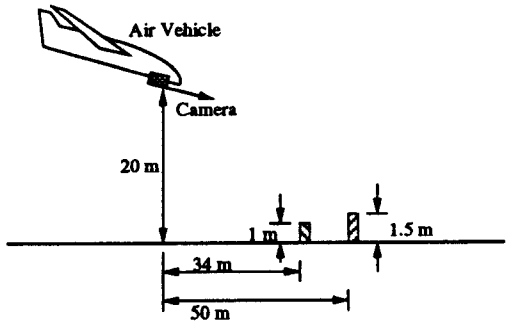


Fig. 7a Side view of terrain with two protrusions

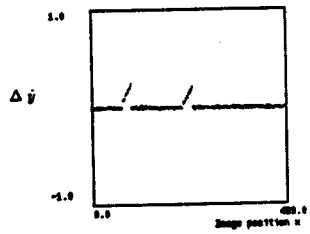

Fig. 7b $\Delta\ \dot{y}$ vs. $x$ in experiment 2 ( 5 % noise )

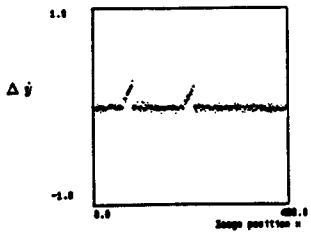

Fig. 7c $\Delta\ \dot{y}$ vs. $x$ in experiment 2 ( 10 % noise )

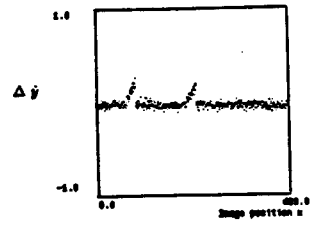

Fig. 7d $\Delta\ \dot{y}$ vs. $x$ in experiment 2 ( 15 % noise )

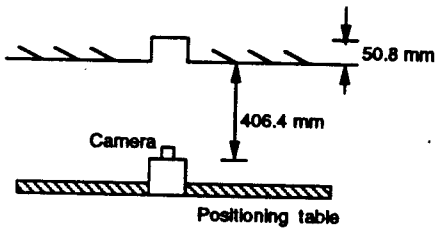


Fig. 8a Top view of the experimental setup in experiment 3

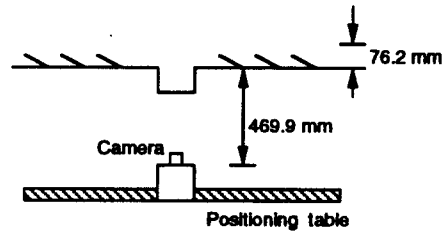


Fig. 9a Top view of the experimental setup in experiment 4

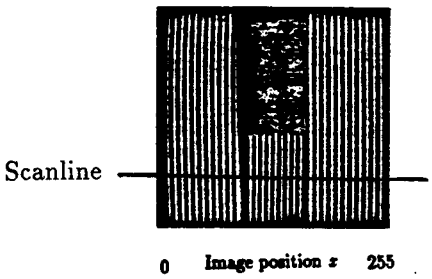


Fig. 8b Original image in experiment 3 only data from the single scanline indicated are used

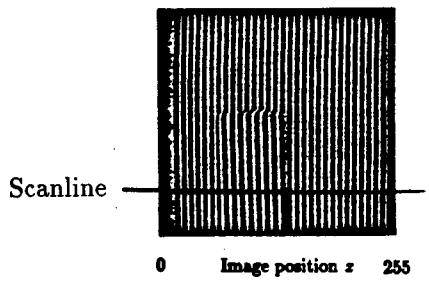


Fig. 9b Original image in experiment 4 only data from the single scanline indicated are used

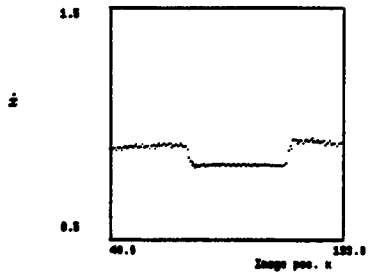


Fig. 8c $\dot{x}$ vs. $x$ in experiment 3

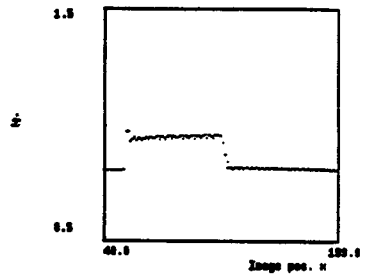


Fig. 9c $\dot{x}$ vs. $x$ in experiment 4

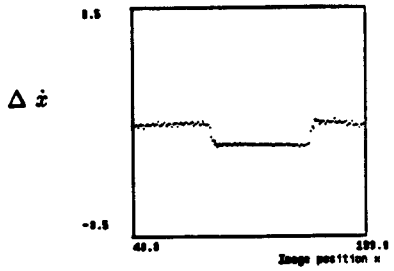


Fig. 8d $\Delta\ \dot{x}$ vs. $x$ in experiment 3

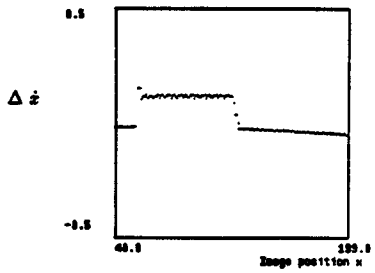


Fig. 9d $\Delta\ \dot{x}$ vs. $x$ in experiment 4